# A stochastic movement model reproduces patterns of site fidelity and long-distance dispersal in a population of Fowler's Toads (*Anaxyrus fowleri*)

Philippe Marchand*, National Socio-Environmental Synthesis Center (SESYNC), Annapolis, MD 21401, United States.

Morgan Boenke, Department of Biology, McGill University, Montreal, Quebec H3A 1B1, Canada.

David M. Green, Redpath Museum, McGill University, Montreal, Quebec H3A 0C4, Canada.

* Corresponding author: marchand.philippe@gmail.com. ORCID: 0000-0001-6717-0475.

**Abstract**

Although amphibians typically exhibit high site fidelity and low dispersal, they do undertake rare, long-distance movements. The factors influencing these events remain poorly understood, partly because amphibian spring movements tend to radiate from breeding sites and the animals are often difficult to locate at other times of the year. In this study, we investigate whether these movement patterns can be reproduced by a parsimonious model where foraging steps follow a heavy-tailed, Lévy alpha-stable distribution and individuals may either return to a previous refuge site or establish a new one. We consider three versions of the return behaviour: (1) a distance-independent probability of return to any previous refuge; (2) constant probability of return to the nearest refuge; or (3) a distance-dependent probability of return to each refuge. Using approximate Bayesian computation, we fit each version of the model to radiotracking data from a population of Fowler's Toads, which inhabits a linear sand dune habitat on the north shore of Lake Erie in Ontario, Canada. Only the model with distance-independent, random returns provides a good fit of the inter-refuge distance distribution and the number of refuges visited per toad. Our results suggest that while toads occasionally forage over long distances, the establishment of new refuges is not driven by the minimization of energy expenditure.

Keywords: amphibian; animal movement; approximate Bayesian computation; foraging; Lévy walk; radiotracking

## 1. Introduction

The movements that individual animals undertake to go from place to place are fundamental to virtually every aspect of animal ecology and behaviour. How small movements of animals at daily or hourly scales result in such larger phenomena as home-ranges, dispersal and migrations at seasonal, annual or life-time scales, however, remains a difficult problem to understand. It has commonly been observed that a high-frequency of short-distance movements combined with rare, long-distance movement events results in a movement step size distribution that is strongly leptokurtic, with a sharper peak and longer tails than expected of a normal distribution, and possibly heavy-tailed, i.e. with the long-distance probability tail extending past that of an exponential distribution (e.g., Cecala et al., 2009; Gomez and Zamora, 1999; Morales, 2002; Paradis et al., 1998; Skalski and Gilliam, 2000). Such heavy-tailed distributions in animal movement may be consistent with the Lévy flight foraging hypothesis (Viswanathan et al., 1999), according to which optimal search patterns follow a power-law distribution of step sizes, with the frequency of steps proportional to some inverse power of their length. However, tests of this hypothesis have been the subject of numerous statistical challenges (Edwards, 2011).

In actuality, animal movement is not scale-free and must be constrained by biological limits, so that the power-law distribution can only hold within a certain range of step sizes (Benhamou, 2007). Over the longer time scales that encompass multiple individual movements, such as may occur during foraging or dispersal behaviours, movement distances may also depend on the animal's memory and "cognitive map" of the environment, features that are poorly represented in movement models based on independent steps (Gautestad and Mysterud, 2013). More complex models that can accommodate both specific movement rules and memory effects

may be required, but their outcomes may not be expressible in terms of analytical likelihood functions.

Although the absence of a likelihood function previously precluded formal statistical analysis, computational and statistical advances in the last 20 years have made it possible to derive inferences from simulation-based models (Hartig et al., 2011). Approximate Bayesian computation (ABC) is a simulation-based inference method originally developed in the field of population genetics, wherein the large number of possible genetic histories and intermediate states leading to a given outcome make explicit likelihood calculations intractable (Beaumont et al., 2002). Since analogous challenges, i.e. path dependence and a large number of unobserved intermediate states, are also encountered in the study of animal movement, ABC provides a flexible mean to test foraging and dispersal behaviour models with empirical data (Marchand et al., 2015).

Anuran amphibians, although they have generally been considered poor dispersers relative to larger, more vagile terrestrial vertebrates, can be valuable subjects for testing models of animal movement. Individuals may show a high level of site fidelity yet mark-recapture studies have also shown that anurans will undertake relatively rare long-distance movements of up to a few km in a matter of days, or as far as 35km over the course of a season (Smith and Green, 2005, 2006). Whether site fidelity is advantageous should depend on the tradeoff between the benefit of a known location relative to the cost of returning to that location (Wells, 2007). As many amphibian species make use of refuge sites as part of their daily activity cycles, this makes discretizing movement simpler as time periods between movement steps are more or less standardized and biologically meaningful. Nevertheless, locating individual anurans outside

of the breeding season can be difficult with many species as they tend to be mostly nocturnal foragers that hide during the daytime. Moreover, the small size of most species precludes the use of GPS satellite telemetry methods that can provide long-term, high-resolution movement time-series for larger terrestrial animals (Wikelski et al., 2007). Both of these difficulties can be overcome, however, with the appropriate model species.

In this study, we develop a parsimonious model that describes both site fidelity and long-distance movements, and apply this model to the movements of Fowler's Toads (*Anaxyrus fowleri*) in a population inhabiting a linear sand dune habitat on the north shore of Lake Erie in Ontario, Canada. In this environment, adult Fowler's Toads are readily locatable as they forage on the beaches at night (Greenberg and Green, 2013). Previous capture-mark-recapture data (Smith and Green 2005, 2006) have established and quantified the heavy-tailed movement distribution curve of these toads. The toads can also be fitted with small radio-transmitters (Boenke, 2011), which allow them to be tracked to their daytime hiding places in the sand dunes fronting the beaches. Based on this radiotracking data, we use ABC to estimate the parameters of the movement model, including the scale and shape of a Lévy-stable distribution of movement steps and the probability of returning to a known refuge rather than establishing a new one.

To assess the importance of energy constraints on movement, we compare the relative fit of three versions of the return step: (1) toads return to a randomly selected previous refuge, independent of distance; (2) they return to the nearest refuge from their current location; or (3) the probability of return to any previous refuge is a decreasing function of the distance to that refuge. We hypothesize that either of the last two models would provide a better fit if minimizing energy expenditure were the primary factor determining refuge choice.

## 2. Methods

### *2.1. Study site and population*

We studied the movement ecology of Fowler's Toads at Long Point in Ontario, Canada, along the beaches of Long Point Provincial Park and the Long Point National Wildlife Area Thoroughfare Point Unit (UTM zone 17 N: 550700 – 553000 Easting, 4713615 – 4714200 Northing; NAD 83 Datum). Although the dune ecosystems along the north shore of Lake Erie are highly dynamic (Gelinas and Quigley, 1973; Stenson, 1993), human disturbance at this site is minimal and movement by toads not constrained either by lack of suitable habitat or by lack of connectivity between habitat patches (Smith and Green, 2005, 2006). The toads generally take refuge in the sand dunes fronting the beach during the day and emerge to forage for invertebrate prey along the lakeshore at night.

### *2.2. Stochastic movement model*

To reflect both the high rate of apparent site fidelity and the heavy-tailed distribution of dispersal steps present in the previous mark-recapture data (Smith and Green, 2006), we used a variant of the multiscaled random walk (MRW) model proposed by Gautestad and Mysterud (2005). The MRW is based on a power-law step length distribution, but differs from a classic Lévy flight by allowing a certain frequency of return steps, wherein the individual revisits a location chosen at random from previous points in the walk. As each successive visit to a location increases its effective weight for future return steps, the MRW model allows home range patterns to emerge without the need to specify an *ad hoc* homing process.

In our model, we assumed that return steps only occurred at the end of the nighttime foraging path, when the toad is at a position $\Delta x_n$ away from the previous day's refuge site. At this point, the toad either takes refuge at its current position or returns to a known refuge site.

*2.2.1. Return steps*

Our three model versions differ in how they describe the return behaviour:

Model 1 (random return): The probability of return is constant ($p_{\text{ret}} = p_0$), and the toad selects a refuge at random from all the previous days' refuges. As in Gautestad and Mysterud's model, multiple visits to a refuge increase its "weight" for future return steps.

Model 2 (nearest return): The probability of return is constant ($p_{\text{ret}} = p_0$), but the toad always returns to the nearest refuge.

Model 3 (distance-based return probability): The probability of returning to a given site decays exponentially with the distance $d_i$ to that refuge:

$$p_{ret(i)} = p_0 e^{\frac{-d_i}{d_0}} \quad , \qquad (1)$$

where $d_0$ is a characteristic distance to be estimated along with $p_0$. The probability of not returning to any previous site is the product of the complements of the $p_{\text{ret(i)}}$ :

$$1 - p_{ret} = \prod \left(1 - p_{ret(i)}\right) \quad , \qquad (2)$$

where $R$ is the number of *distinct* previous refuges.

In the case of a return event, the probability of each refuge being chosen is given by:

$$P\left(return\ at\ i \middle| return\right) = \frac{p_{ret(i)}}{\sum p_{ret(i)}} \quad . \ (3)$$

With an additional parameter, the third model allowed us to consider intermediate cases of distance-dependence. As the characteristic distance $d_0$ decreases, it becomes increasingly

likely that the toad will choose the nearest refuge; yet the outcome differs from that of model 2, since the probability of return is not constant but decreases with distance. In the limit where $d_0$ is very large, $p_{ret(i)} = p_0$ and all previous sites have the same probability of return. Contrary to model 1, however, the probability of returning to any site is not constant but increases with $R$ (as a consequence of Eq. 2). Moreover, since model 3 considers distinct refuge sites, multiple visits to the same refuge do not increase its probability weight.

*2.2.2. Overnight displacement*

The net overnight displacement, $\Delta x_n$, in the model followed a symmetric, zero-centered stable (a.k.a. Lévy alpha-stable) distribution, $S(\alpha, \gamma)$, with stability parameter $\alpha$ ($0 < \alpha \leq 2$) and scale parameter $\gamma > 0$. With $\alpha = 2$, the stable distribution reduces to a normal law, whereas decreasing values of $\alpha$ produced increasingly leptokurtic (i.e. heavy-tailed) distributions, including the Cauchy distribution ($\alpha = 1$) as a special case (Uchaikin and Zolotarev, 1999). For $\alpha < 2$, the tails of the probability density followed a power law decay with exponent $-(1 + \alpha)$.

Although there is no closed form of the stable probability density for arbitrary $\alpha$, random draws from $S(\alpha, \gamma)$ can be generated by the CMS algorithm (Chambers *et al*. 1976):

$$S = \gamma \frac{\sin \alpha U}{(\cos U)^{\frac{1}{\alpha}}} \left[ \frac{\cos\left((1-\alpha)U\right)}{W} \right]^{\frac{1-\alpha}{\alpha}}, \qquad (4)$$

where $U$ is a uniformly distributed angle in $(-\pi, \pi)$ and $W$ has a standard exponential distribution.

A key property of the stable distribution is that the sum of stable random variables is also stable; in particular, the sum of $N$ independent variables distributed as $S(\alpha, \gamma)$ is stable with the

same stability parameter α and a scale $\gamma_N = N^{1/\alpha}\gamma$. Furthermore, the generalized central limit theorem of Gnedenko and Kolmogorov (1954) shows that the sum of independent variables following a common distribution with asymptotic power-law tail converges to a stable distribution.

Given these properties, our assumption that $\Delta x_n$ has a stable distribution was robust to differences in the small-scale foraging behaviour. For example, while foraging steps are probably correlated on a short-term scale, as long as there is some intermediate time scale where successive displacements can be modelled as independent and following a heavy-tailed (power-law) distribution, the stable distribution will be a reasonable approximation of net displacement.

### *2.3. Model fitting with approximate Bayesian computation*

We fitted our model by approximate Bayesian computation (ABC) using the ABC-rejection algorithm, as implemented in the 'abc' package (Csilléry et al., 2012) in R (R Core Team, 2016). Consider a simulation model that takes an input parameter vector $\theta$ and outputs a vector of summary statistics ($S$) calculated from the simulation outcome. Given a set of $\theta$ vectors, drawn from the parameters' prior distributions, and a corresponding set of simulation outputs $S(\theta)$, ABC-rejection simply selects a subset of $\theta$ for which the output statistics are close to those of the observed data $D$, i.e. where $d[S(\theta), S(D)] < \varepsilon$ for a chosen distance function $d$ and tolerance level ε. The selected subset approximates the joint posterior distribution of $\theta$. The approximation accuracy can be further improved by fitting a local-linear regression model of $\theta$ vs. $S(\theta)$ and using that empirical model to correct each $\theta$ towards the value it would have at $S(D)$ (Beaumont et al., 2002).

The ABC-rejection algorithm can be naturally extended to the problem of model selection by treating the choice of model as a discrete parameter (Toni et al., 2009). If the number of simulations run under each model is proportional to its prior probability, then the representation of a model among the simulations retained following the rejection step is an estimate of its posterior probability. As in the parameter estimation case, the approximation can be improved by fitting a regression of the discrete model probabilities, i.e. a multinomial logistic regression, as a function of the summary statistics in the vicinity of the observed statistics (Beaumont, 2008).

The main drawback of ABC-rejection is the high number of simulations necessary to get a sufficient number of results in the vicinity of the data. Alternative ABC algorithms use Markov chain Monte Carlo or sequential Monte Carlo (a.k.a. particle filter) methods to gradually concentrate the sampling effort in the areas of high-agreement between simulated and observed statistics (Marjoram et al., 2003; Sisson et al., 2007). Yet, ABC-rejection has the advantage of decoupling the simulation and estimation steps, which allows the entire set of simulations to be run ahead of time and, possibly, in parallel on a high-performance computing cluster. Multiple estimations can then be performed from this set of simulation outputs, which is especially helpful when performing cross-validation.

*2.3.1. Prior distributions and summary statistics*

Our results were based on 10,000 simulations of each version of the stochastic model. For each simulation, we drew parameters from the following uniform prior distributions: $\alpha \sim U(1, 2)$, $\gamma \sim U(10\text{m}, 100\text{m})$, $p_0 \sim U(0, 1)$ and (for model 3 only) $d_0 \sim \text{U}(20\text{m}, 2000\text{m})$. To match the size and structure of the observed dataset, we simulated the movement of 66 toads over 63 days, then

subset the results to keep only the (Toad, Day) observation points present in the data. For each of four different time lags (1, 2, 4 and 8 days), we calculated three statistics over all pairs of points with the same toad and the corresponding time lag: (1) the frequency of returns (defined as $|\Delta x|<$ 10m), as well as (2) the mean and (3) standard deviation of $\log (\Delta x)^2$ for non-returns, over all pairs of points with the same toad and corresponding time lag. We chose these 12 summary statistics as well as the 10m distance threshold to capture the key characteristics of the empirical distribution of relocation distances at multiple time scales (see section 3.1 and Fig. 1). We used the Euclidean distance (sum of squared differences) to compare this vector of summary statistics to the corresponding statistics of the radiotracking data.

*2.3.2. Cross-validation*

We used the 'abc' package's cross-validation feature to verify the identifiability of our model, i.e. determining whether the size of the dataset and the chosen summary statistics are sufficient to estimate the parameters of interest for each model version, and distinguish the outcome of the alternate model versions. We also used cross-validation to choose an optimal tolerance rate, which is the fraction of best-fitting simulations to keep for estimating the posterior distribution.

For the parameter estimation problem, cross-validation was performed separately for each model version. Taking one of the simulation results as the "data", we applied ABC to estimate the true parameters of that simulation based on the remainder of the simulation results. We repeated this process for 100 sampled simulation results and four different tolerance rates (0.5%, 1%, 5% and 10%). The cross-validation accuracy was quantified using the relative

estimation error, defined as the mean square difference between estimated and true parameter values divided by the variance of the true values over the 100 sampled simulations.

For the model selection problem, cross-validation consisted in taking one simulation output as the data and applying ABC to the remaining 29,999 simulation results (combined from all three models) to estimate the posterior probabilities of each model version. We repeated this process for 100 sampled simulations per model version, using the same tolerance rates as above. Model selection accuracy is quantified by the misclassification rate: the fraction of cases where the model version with the highest posterior probability differed from the true model.

*2.3.3. Parameter estimates and model selection*

We estimated the posterior distribution of each parameter via ABC-rejection, using the tolerance rate selected by cross-validation and applying the local-linear regression correction of Beaumont et al. (2002). For the regression correction, we applied a logit transformation to the stability parameter (α) to keep the inferred values within the (1, 2) bounds, and a log transformation to $d_0$ to constrain its range to positive values. Parameters were estimated separately for the three versions of the model.

To compare the fit of the different model versions, we first estimated the posterior probabilities of the three models by ABC-rejection, followed by multinomial logistic regression of model probabilities in the vicinity of the observed summary statistics (Beaumont 2008). We then verified that simulation outputs from the fitted version of each model (with parameters drawn from their posterior distribution) could reproduce the observed summary statistics.

As an additional posterior predictive check, we compared the number of distinct refuge sites in the simulated and observed datasets. In practice, we defined this quantity as the number of clusters obtained at a distance threshold of 10m, when performing hierarchical clustering of the point locations using the complete-linkage method ('hclust' function in R). The complete-linkage criterion ensures that each pair of points in the cluster is separated by no more than the specified distance threshold.

### *2.4. Radiotracking data*

We collected radiotracking data on Fowler's Toads at our study site during mid-June to late August of 2009 and 2010 (Boenke, 2011). Toads were captured opportunistically while they were foraging on the beach, and outfitted with either Holohil BD-2 (in 2009) or BD-2N (in 2010) radiotransmitters, which were attached to the toad via a filament covered in plastic tubing (following Bartelt and Peterson, 2000). The total weight of the transmitter and harness (ca. 2 g) constituted ~5% of the typical adult toad weight, and in no case exceeded 10% of the individual's weight, as recommended by Rowley and Alford (2007). Toads were tracked with an HR2600 Osprey Receiver (H.A.B.I.T. Research, Victoria, BC, Canada) and Yagi 3-element antenna. Upon finding each toad, its position was recorded with a Magellan Mobile Mapper 6 GPS unit (Magellan Navigation, Inc., Santa Clara, CA, USA). The location of each tracked toad was recorded at least once per night (active foraging) and once per day (resting in refuge) but we only used the daytime locations in the present study. The number of consecutive days in a tracking bout varied by toad, as some individuals shed their transmitter, or else it had to be removed to alleviate skin irritation. Since individuals were identified by toe clipping or

distinctive marks from digital photographs, toads that lost their transmitter could sometimes be retrieved, allowing multiple tracking bouts per toad (Boenke, 2011). All procedures with animals were conducted under McGill University Animal Use Protocol No. 4569.

The position of toads' daytime refuges relative to the shore is governed by tradeoffs between wave avoidance, predator avoidance, elevation and proximity to water (Boenke, 2011). In contrast, movement along the shoreline is unconstrained, meaning that dispersal occurs mostly along a single dimension. For this reason, we projected all refuge locations on a single axis, obtained by linear regression of the two-dimensional coordinates, and only modeled this one-dimensional component of toad movement.

### *2.5. Source code and data access*

The dataset used for this study and the R code for all simulation and analyses can be downloaded from GitHub: http://github.com/pmarchand1/fowlers-toad-move/.

## 3. Results

### *3.1. Empirical distribution of relocation distances*

The radio-tracking dataset included 66 toads, with between 2 and 30 daytime points recorded, for a mean of 12 locations per toad per season.

When shown on a logarithmic scale (Fig. 1), the distribution of distances between daytime refuges of a toad was characterized by a symmetric peak combined with an inflated number of low-distance events. Given the GPS margin of error of 3 – 5m per point, distances of less than 10m could not be measured reliably (Boenke, 2011). Therefore, the excess probability

in that part of the distribution would be consistent with toads returning to previous sites. In contrast with the expectations of a random walk model, where the whole distribution would shift to larger distances as the time step increases, the peak of relocation distances varied little between time lags of 1 to 8 days. Instead, longer time lags increased the total probability on the high end of the distribution as the fraction of short-distance (or return) events decreased.

### *3.2. Approximate Bayesian computation*

#### *3.2.1 Cross-validation*

With the exception of $d_0$ in model 3 (see below), the cross-validation results (Table S1 in the supplementary data) showed a good agreement between the true values of the parameters and their posterior median estimated via ABC. Overall, the relative estimation error was minimized with a 5% tolerance level; the supplementary Fig. S1 shows how the estimated and true values compare across all parameters at that tolerance level. For all three model versions, the relative error was higher for α (10% to 14%) than for γ (around 7%) or $p_0$ (1% to 5%). Since α determines the power-law tail of the stable distribution, its value is sensitive to rare, long-distance events, which could explain the higher estimation variance. The characteristic distance $d_0$ had the highest estimation error, at over 60% of the prior range. Therefore, this parameter might only be identifiable with a larger dataset.

The ABC model selection algorithm could discriminate well between Model 2 and either other version. However, 35% of the Model 1 runs were misidentified as Model 3 and 23% of Model 3 runs were misidentified as Model 1 (Table 1). This is consistent with the behaviour of Model 3 approaching random returns in the limit of high $d_0$; while there are still differences

between the two models in that limit, they might not be detectable with the chosen summary statistics.

*3.2.2. Parameter estimation*

The posterior median and 95% Bayesian credible interval for all parameter estimates are shown in Table 2. The estimates of the stable distribution parameters were similar for Model 1 ($\alpha = 1.7$, $\gamma = 34$ m) and Model 3 ($\alpha = 1.65$, $\gamma = 32$ m), whereas both values were higher for Model 2 ($\alpha = 1.83$, $\gamma = 46$ m).

The estimated values of $\alpha$ suggest a power-law tail with an exponent between $-2.6$ and $-2.8$. The estimates of $\alpha$ could be biased upwards, however, since long-distance dispersal events are more likely to take toads outside of the tracking range. That is, the power-law tail could extend further than inferred from the data.

As expected based on the poor cross-validation results, the estimate of $d_0$ in model 3 has a very wide credible interval (220 to 1697 m). In comparison, the largest distance between any two observations of the same toad in the dataset was 1198 m, and only 4 out of 66 toads visited locations more than 350 m apart. Most of the posterior distribution thus lies in the high $d_0$ range where refuge choice is not primarily constrained by distance. Note that the estimates of $p_0$ in Model 3 (0.43) and Model 1 (0.60) are not directly comparable even in the distance-independent case, since the actual probability of return in Model 3 increases with the number of visited refuges (see section 2.2).

We verified that our posterior parameter estimates did not significantly change when performing additional simulations beyond the current 10,000 per model version (Fig. S2 in the supplementary data).

*3.2.3. Model selection*

The ABC model selection process resulted in posterior probabilities of 15% for Model 1 (random return), 0% for Model 2 (nearest return) and 85% for Model 3 (distance-dependent return probability). Given the high probability of misclassification between Model 1 and 3 (Table 1) and the difference in complexity between the two models (3 versus 4 adjustable parameters), this result alone does not provide strong evidence of a better fit for Model 3.

The comparison of observed and simulated summary statistics from the three models, with simulation parameters drawn from their respective posterior distribution, shows that Model 2 is too dispersive. That is, the mean log distance increases – and the probability of return decreases – too rapidly with greater time lags. In contrast, the range of simulated results from Models 1 and 3 is consistent with the observed statistics at all time lags (Fig. 2).

Finally, we computed the number of distinct refuge sites, defined in section 2.3 as clusters of points with diameter less than 10m, for each toad in both the empirical data and the output of each simulation model (with parameters drawn from their posterior distribution). This quantity is strongly dependent on the number of observations by individual; our results show that this relationship can be well approximated by a linear regression on a log-log plot (Fig. 3). Note that the simulation results show less variance as they represent the average of 500 simulated paths by toad. This number of refuges statistic, which wasn't directly used in fitting the parameters of each model, shows a better fit for Model 1: the 95% confidence intervals of the regression lines for observed and simulated points overlap. Model 3, in contrast, results in too few distinct refuges for toads with many observations. This may be due to the functional form of

the probability of return in this model (Eq. 2), which increases with the number of distinct refuges already visited.

## 4. Discussion

In the analysis above, we showed that a parsimonious model of foraging behaviour (our Model 1) successfully reproduced the main patterns of refuge site fidelity and relocation among a population of Fowler's Toads. The model assumed that the net displacements of toads during nighttime foraging follows a heavy-tailed, Lévy-stable distribution, and that toads may either take refuge at the end of their foraging path, or return to a random refuge among those previously visited.

The assumption that toads returning to a previous refuge choose one at random may seem unrealistic. Yet it fit the data better than two alternative models we tested, where the probability of return and/or the choice of refuge were distance-dependent. It might be that movement cost is only one of many factors determining refuge selection, along with slope, elevation and vegetation cover of potential refuge sites (Boenke, 2011). Without knowing the spatial structure of these microhabitat variables along the beach length, it is difficult to determine how they could affect the movement statistics. Even if additional environmental data were available, the size of the tracking dataset (individuals and locations per individual) would also set a limit to the complexity of verifiable models: the very diffuse posterior distribution for the characteristic distance $d_0$ in model 3 provides a good example of this problem.

Even for this simple model, this study illustrates the power and flexibility of approximate Bayesian computation for the calibration and testing of mechanistic movement models from field

data. In particular, ABC doesn't require the stochastic process of interest to have a known analytical likelihood, and it can easily accommodate gaps in observations (by subsetting the simulated data) as well as sources of error and censoring. In this study, we took into account the unreliability of GPS measurements at short distances, and if we had an independent measure of long-distance censoring, that effect could have been included as well.

Our results indicate that long-term movement patterns, such as dispersal, may be profoundly affected by small-scale micro-habitat choices and day-to-day movement. Sand dunes and beaches are highly dynamic environments that are strongly affected by both weather conditions and waves. The large temporal variation in habitat quality, combined with a relatively lower spatial variability in the direction parallel to the shore, matches conditions that have been found to favor heavy-tailed movement patterns (Lowe, 2009). Temporal habitat variability can also contribute to the decrease in the probability of return with larger time steps, as preferable refuge locations shift during the season.

This stochastic movement model, calibrated through individual-level tracking data, provides a measure of home range size that is robust to changes in the scale or number of observations. We note that while the number of refuges sites utilized by a toad increases with the number of observation days, the median relocation distance (the peak on the log scale of Fig. 1) varies little with time. This suggests that most toads' movement remains within that spatial range. Conversely, the probability of rare, long-distance dispersal events predicted by the model can serve to estimate the level of connectivity between toad populations separated by a given distance along the shore.

**Acknowledgements**

We thank the Canadian Wildlife Service and Ontario Parks for permission to study toads at Long Point and J. Middleton, E. Dirse, R. Card, S. Bosco Y.-T. Huang, S. Price, A. Merck, J. Krohner, M. Warren-Paquin and G. Thomas, for field assistance. This research was funded by grants from NSERC Canada, World Wildlife Fund Canada, Ontario Ministry of Natural Resources and Forestry, Wildlife Preservation Canada, and the Canadian Wildlife Federation. P. Marchand received support from the National Socio-Environmental Synthesis Center (SESYNC) under funding received from the National Science Foundation (NSF) [grant number DBI-1052875].

**Literature Cited**

Bartelt, P.E. and Peterson, C.R. 2000. A description and evaluation of a plastic belt for attaching radio transmitters to western toads (*Bufo boreas*). – *Northwest. Nat.* **81**: 121–128.

Beaumont, M.A., Zhang, W. and Balding, D.J. 2002. Approximate Bayesian computation in population genetics. – *Genetics* **162**: 2025–2035.

Beaumont, M. A. 2008. Joint determination of topology, divergence time, and immigration in population trees. – In: Matsumura, S., Forster, P. and Renfrew, C. (eds.) Simulation, genetics, and human prehistory. McDonald Institute for Archaeological Research, Cambridge.

Benhamou, S. 2007. How many animals really do the Lévy walk? – *Ecology* **88**: 1962–1969.

Boenke, M. 2011. Terrestrial habitat and ecology of Fowler's toads (*Anaxyrus fowleri*). – M.Sc. thesis, Department of Biology, McGill University, Montreal, Canada.

Bradford, D.F. 2005. Factors implicated in amphibian population declines in the United States. – In: Lannoo, M.J. (ed.), Amphibian declines: the conservation status of United States species. Univ. of California Press.

Cecala, K.K., Price, S.J. and Dorcas, M.E. 2009. Evaluating existing movement hypotheses in linear systems using larval stream salamanders. – *Can. J. Zool.* **87**: 292–298.

Chambers, J.M., Mallows, C.L. and Stuck, B.W. 1976. A method for simulating stable random variables. – *J. Am. Stat. Assoc.* **71**: 340–344.

Clarke, R.D. (1974). Activity and movement patterns in a population of Fowler's toad, *Bufo woodhousei fowleri. American Midland Naturalist* **92:** 258-274.

COSEWIC (2010). COSEWIC assessment and status report on the Fowler's Toad *Anaxyrus fowleri* in Canada. – Committee on the Status of Endangered Wildlife in Canada. Ottawa. vii + 58 pp. (www.sararegistry.gc.ca/status/status_e.cfm).

Csilléry, K., François, O. and Blum, M.G.B. 2012. abc: An R package for approximate Bayesian computation (ABC). – *Methods Ecol. Evol.* **3**: 475–479.

Edwards, A.M. 2011. Overturning conclusions of Lévy flight movement patterns by fishing boats and foraging animals. – *Ecology* **92**: 1247–1257.

Gautestad, A.O. and Mysterud, I. 2005. Intrinsic scaling complexity in animal dispersion and abundance. – *Am. Nat.* **165**: 44–55.

Gautestad, A.O. and Mysterud, I. 2013. The Lévy flight foraging hypothesis: forgetting about memory may lead to false verification of Brownian motion. – *Mov. Ecol.* **1**:9.

Gelinas, P.J. and Quigley, R.M. 1973. The influence of geology on erosion rates along the north shore of Lake Erie. – In: Proc. Sixteenth Conf. Great Lakes Res., Int. Assoc. Great Lakes Res. 421–430.

Gnedenko, B.V. and Kolmogorov, A.N. 1954. Limit distributions for sums of independent random variables. – Addison-Wesley.

Gomez, J.M. and Zamora, R. 1999. Generalization vs. specialization in the pollination system of *Hormathophylla spinosa* (Cruciferae). – *Ecology* **80**: 796–805.

Green, D.M. 2005. *Bufo fowleri*, Fowler's toad. – In: Lannoo, M.J. (ed.), Amphibian declines: the conservation status of United States species. Univ. of California Press.

Green, D. M., A. R. Yagi, and S. E. Hamill. 2011. Recovery Strategy for the Fowler's Toad (*Anaxyrus fowleri*) in Ontario. – Ontario Recovery Strategy Series. Ontario Ministry of Natural Resources, Peterborough, Ontario. vi + 21 pp.

Greenberg, D.A. and Green, D.M. 2013. Effects of an invasive plant on population dynamics in toads. – *Conserv. Biol.* **27**: 1049–1057.

Hartig, F., Calabrese, J.M., Reineking, B., Wiegand, T. and Huth, A. 2011. Statistical inference for stochastic simulation models – theory and application – *Ecol. Letters* **14**: 816–827.

Lowe, W.H. 2009. What drives long-distance dispersal? A test of theoretical predictions. *Ecology* **90**: 1456–1462.

Marchand, P., Harmon-Threatt, A.N. and Chapela, I. 2015. Testing models of bee foraging behavior through the analysis of pollen loads and floral density data. – *Ecol. Model.* **313**: 41–49.

Marjoram, P., Molitor, J., Plagnol, V. and Tavaré, S. 2003. Markov chain Monte Carlo without likelihoods. – *PNAS* **100**: 15324–15328.

Morales, J.M. 2002. Behavior at habitat boundaries can produce leptokurtic movement distributions. – *Am. Nat.* **160**: 531–538.

Paradis, E., Braille, S.R., Sutherland, W.J. and Gregory, R.D. 1998. Patterns of natal and breeding dispersal in birds. – *J. Anim. Ecol.* **67**: 518–536.

R Core Team. 2016. R: A language and environment for statistical computing. R Foundation for Statistical Computing. Vienna, Austria. http://www.R-project.org.

Rowley, J.J.L. and Alford, R.A. 2007. Techniques for tracking amphibians: The effects of tag attachment, and harmonic direction finding versus radio telemetry. – *Amphib.-Rept.* **2007**: 367–376.

Sisson, S.A., Fan, Y. and Tanaka, M.M. 2007. Sequential Monte Carlo without likelihoods. – *PNAS* **104**: 1760–1765.

Skalski, G.T. and Gilliam, J.F. 2000. Modeling diffusive spread in a heterogeneous population: A movement study with stream fish. – *Ecology* **81**:1685–1700.

Smith, M.A. and Green, D.M. 2005. Dispersal and the metapopulation paradigm in amphibian ecology and conservation: are all amphibian populations metapopulations? – *Ecography* **28**: 110–128.

Smith, M.A. and Green, D.M. 2006. Sex, isolation and fidelity: unbiased long-distance dispersal in a terrestrial amphibian. – *Ecography* **29**: 649–658.

Stenson, R. 1993. The Long Point area: An abiotic perspective. – Long Point Environmental Folio Series. Technical Paper #2. Heritage Resources Centre, University of Waterloo. Waterloo, Ontario.

Storfer, A. 2003. Amphibian declines: future directions. – *Divers. Distrib.* **9**: 151–163.

Stuart, S.N., Chanson, J.S., Cox, N.A., Young, B.E., Rodrigues, A.S.L., Fischman, D.L. and Waller, R.W. 2004. Status and trends of amphibian declines and extinctions worldwide. *Science* **306**: 1783–1786.

Tavaré, S., Balding, D.J., Griffiths, R.C. and Donnelly, P. 1997. Inferring coalescence times from DNA sequence data. – *Genetics* **145**: 505–518.

Toni, T., Welch, D., Strelkowa, N., Ipsen, A. and Stumpf, M.P.H. 2009. Approximate Bayesian computation scheme for parameter inference and model selection in dynamical systems. – *J. R. Soc. Interface* **6**: 187–202.

Uchaikin, V.V. and Zolotarev, V.M. 1999. Chance and stability: Stable distributions and their applications. – De Gruyter, Utrecht.

Viswanathan, G.M., Buldyrev, S.V., Havlin, S., da Luz, M.G.E., Raposo, E.P. and Stanley, H.E. 1999. Optimizing the success of random searches. – *Nature* **401**: 911–914.

Wells 2007. The ecology and behavior of amphibians. – Univ. of Chicago Press.

Wikelski, M., Kays, R.W., Kasdin, N.J., Thorup, K., Smith, J.A. and Swenson, G.W. 2007. Going wild: What a global small-animal tracking system could do for experimental biologists. – *J. Exp. Biol.* **210**: 181–186.

## Tables

| | Model 1 predicted | Model 2 predicted | Model 3 predicted |
|---|---|---|---|
| Model 1 true | 62.2% | 3.2% | 34.5% |
| Model 2 true | 8.4% | 88.4% | 3.2% |
| Model 3 true | 22.6% | 3.0% | 74.4% |

Table 1: Confusion matrix for model selection, based on cross-validation results. For each model version, we selected a random subset of 100 (out of 10,000) simulations, considered each one in turn as the "data", and applied the ABC model selection procedure (with a 5% tolerance level) to determine which of the three model versions had the highest probability of being the source of the simulated dataset.

| **Parameter** | | $\alpha$ | $\gamma$ (m) | $p_0$ | $d_0$ (m) |
|---|---|---|---|---|---|
| **Uniform prior range** | | (1, 2) | (10, 100) | (0, 1) | (20, 2000) |
| **Model 1** | Median | 1.70 | 34 | 0.60 | |
| | 95% BCI | (1.41, 1.94) | (26, 42) | (0.53, 0.65) | |
| | CV error | 10.3% | 6.6% | 1.0% | |
| **Model 2** | Median | 1.83 | 46 | 0.65 | |
| | 95% BCI | (1.35, 1.99) | (34, 60) | (0.54, 0.72) | |
| | CV error | 13.6% | 7.6% | 1.3% | |
| **Model 3** | Median | 1.65 | 32 | 0.43 | 758 |
| | 95% BCI | (1.37, 1.91) | (26, 40) | (0.31, 0.59) | (220, 1697) |
| | CV error | 10.0% | 7.0% | 4.8% | 63.1% |

Table 2: Approximate Bayesian computation estimates of the simulation model parameters. Posterior parameter distributions are obtained through selection of the 500 (out of 10,000) best-fitting parameter sets for each model version, followed by a local-linear

regression adjustment. The table shows the median and 95% Bayesian credible interval (BCI) of the parameter's posterior distribution, along with the relative error estimated from cross-validation (CV error).

## Figure captions

Figure 1: Kernel density estimates for the *x*-axis (parallel to shore) distance – shown here on a log scale – between daytime refuges for time lags of 1, 2, 4 and 8 days. We calculated distances between all pairs of fixes separated by the given time lag for each tracked toad. Distances smaller than 10m (indicated by the finely dotted line) are within the GPS margin of error and thus considered return events for the purpose of our model.

Figure 2: Kernel density estimates of the summary statistics from 500 simulations of each movement model, with parameters drawn from the posterior distributions obtained by approximate Bayesian computation. The red lines indicate the summary statistic's value in the observed data.

Figure 3: Number of refuge sites (point clusters of diameter < 10m) as a function of the number of radiotracking observations by toad for the three simulation model versions, compared with the observed data. In each case, we estimate a linear trend on a log-log scale and show the corresponding 95% confidence interval (shaded area). The simulated number of refuges shown for each model version is the mean of 500 model runs with parameters drawn from their posterior distribution.

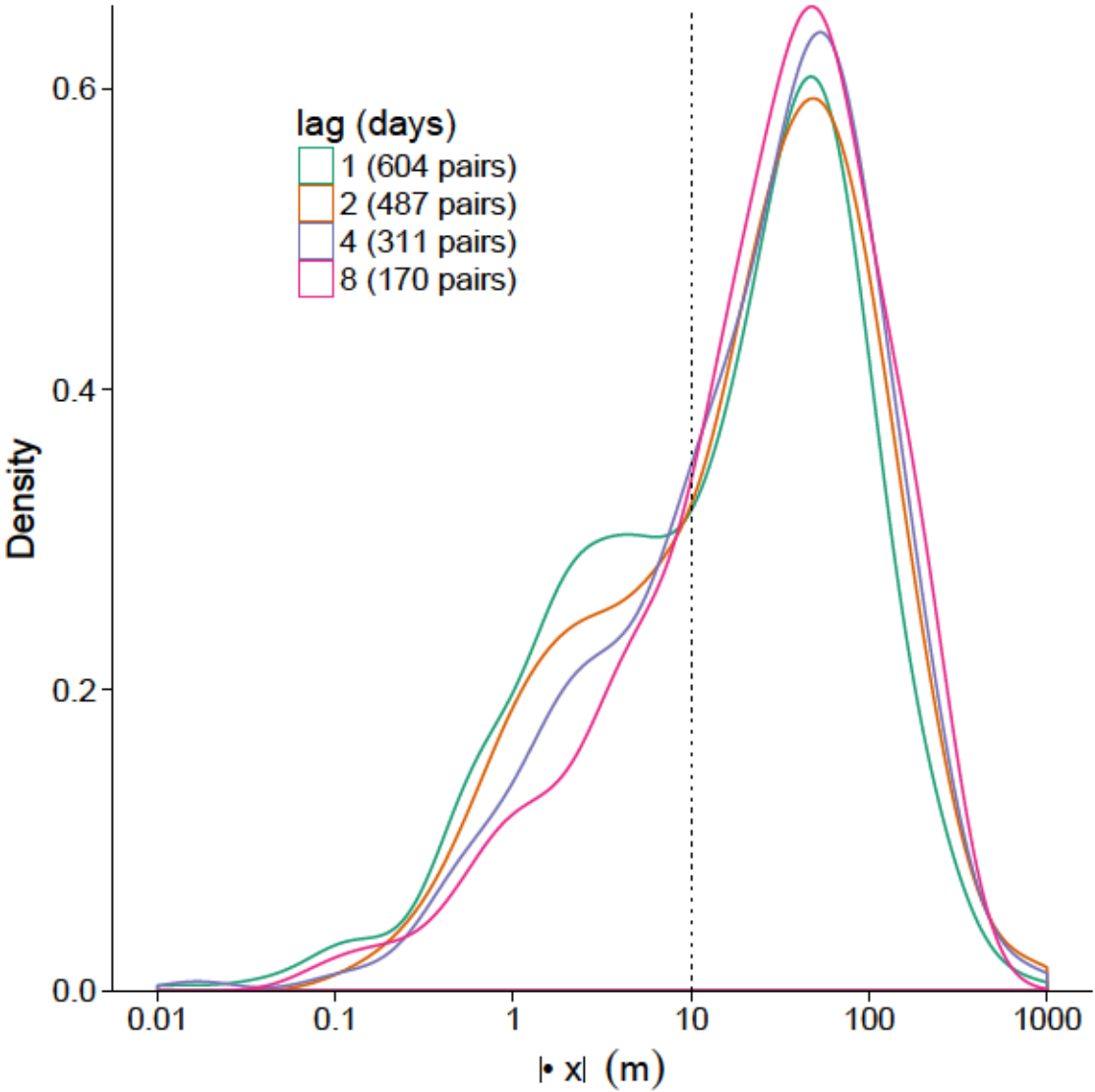
lag (days)
1 (604 pairs)
2 (487 pairs)
4 (311 pairs)
8 (170 pairs)
Density
0.0
0.2
0.4
0.6
0.01
0.1
1
10
100
1000
|• x| (m)

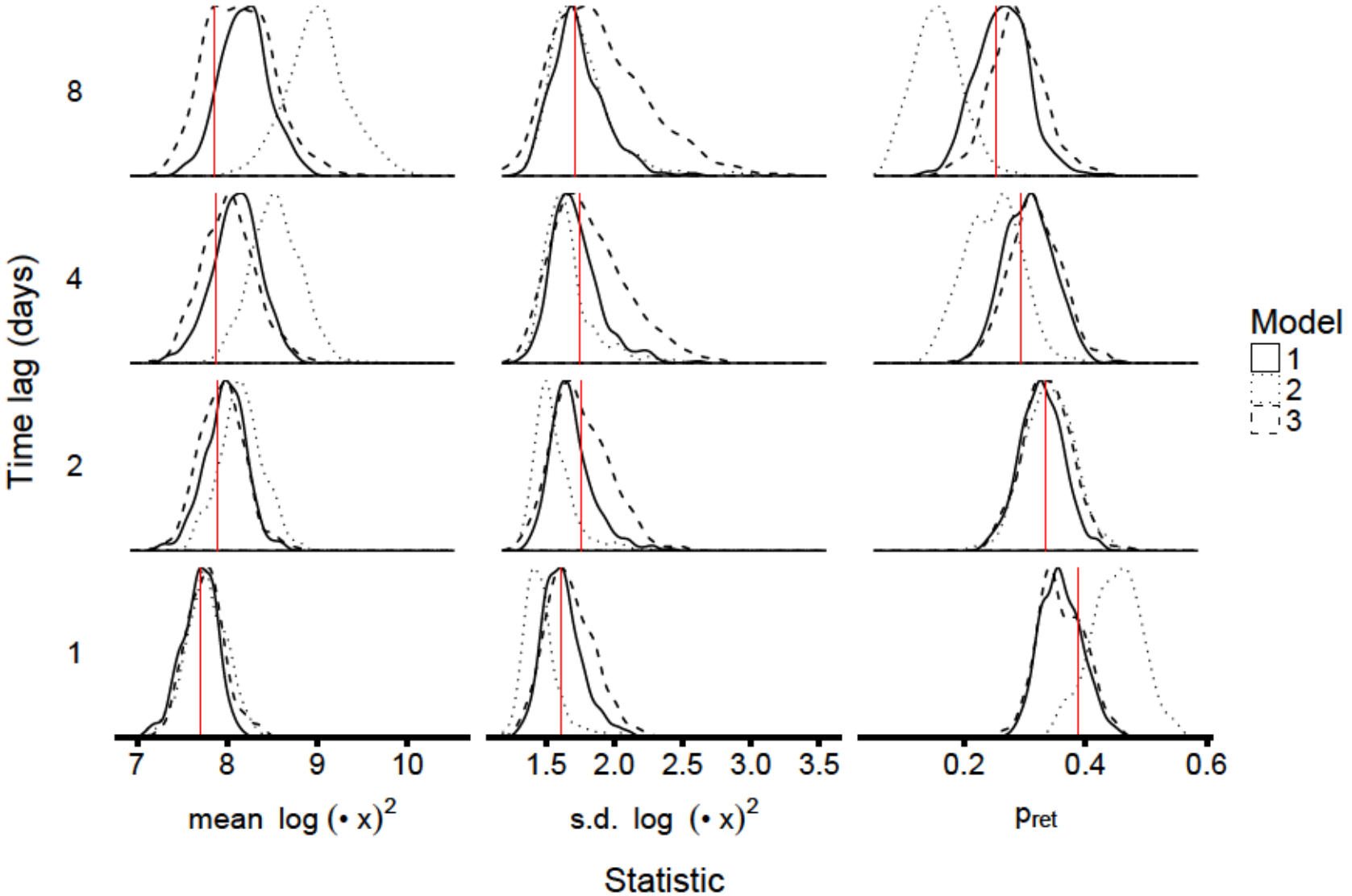
Time lag (days)
8
4
2
1
7
8
9
10
1.5
2.0
2.5
3.0
3.5
0.2
0.4
0.6
mean log (• x)2
s.d. log (• x)2
pret
Statistic
Model
1
2
3

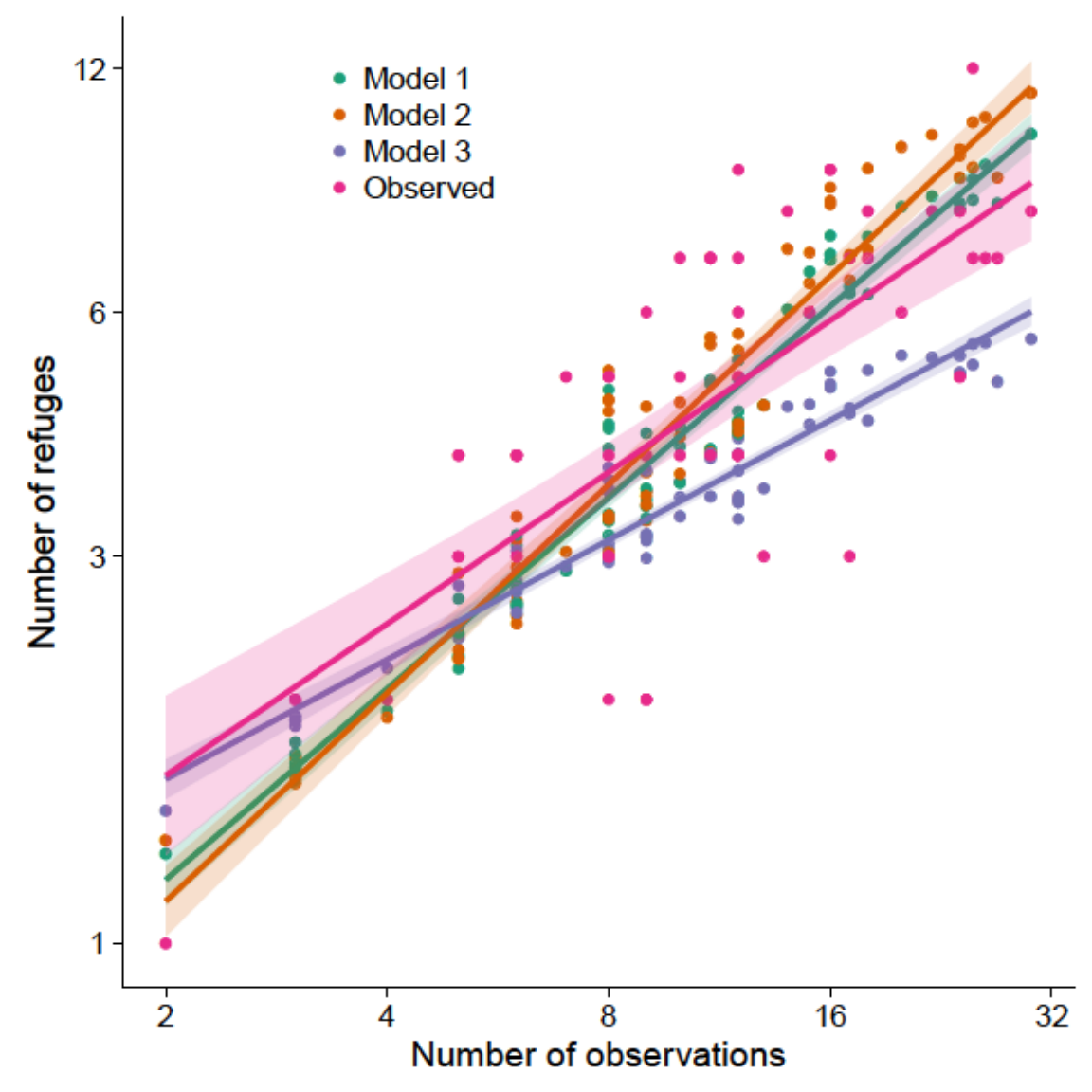
Model 1
Model 2
Model 3
Observed
12
6
3
1
Number of refuges
2
4
8
16
32
Number of observations

**A stochastic movement model reproduces patterns of site fidelity and long-distance dispersal in a population of Fowler's Toads (*Anaxyrus fowleri*)**

## Supplementary table

| Tolerance | Model 1 estimation | | | Model 2 estimation | | | Model 3 estimation | | | | Model selection | | |
|---|---|---|---|---|---|---|---|---|---|---|---|---|---|
| | $\alpha$ | $\gamma$ | $p_0$ | $\alpha$ | $\gamma$ | $p_0$ | $\alpha$ | $\gamma$ | $p_0$ | $d_0$ | Model 1 | Model 2 | Model 3 |
| 0.5% | 16% | 7.1% | 1.3% | 23% | 6.9% | 1.4% | 17% | 12.5% | 6.4% | 94% | 37% | 10% | 31% |
| 1% | 13% | 6.2% | 1.0% | 14% | 7.4% | 1.1% | 12% | 8.4% | 4.7% | 76% | 36% | 11% | 28% |
| 5% | 10% | 6.6% | 1.0% | 14% | 7.6% | 1.3% | 10% | 7.0% | 4.8% | 63% | 38% | 12% | 26% |
| 10% | 11% | 5.6% | 1.2% | 13% | 7.0% | 1.6% | 10% | 7.1% | 5.0% | 63% | 39% | 12% | 27% |

Table S1: Relative estimation and model selection errors calculated by cross-validation, as a function of the tolerance level (% of accepted simulations). The lowest value for each estimate is highlighted. For parameter estimation, the relative error is the mean square difference between the true parameter value and the estimated value, divided by the variance of the true parameter value across the 100 cross-validation replicates. The model selection error for model *i* is the fraction of cross-validation replicates of model *i* where the selected model was not *i*.

**A stochastic movement model reproduces patterns of site fidelity and long-distance dispersal in a population of Fowler's Toads (*Anaxyrus fowleri*)**

## Supplementary figures

Fig. S1. Cross-validation results for the approximate Bayesian computation (ABC) estimation procedure, for (a) Model 1 (random return), (b) Model 2 (nearest return) and (c) Model 3 (distance-based return probability). For each model version, we selected a random sample of 100 (out of 10,000) simulation results, considered each one in turn as the "data" and ran the ABC-rejection algorithm (with 5% tolerance level) on the remainder of the simulation results to infer the true parameter values of the left out simulation. The diagonal line on each plot indicates equality between true and estimated values. The point estimates shown are the median of the posterior distribution, while error bars represent the 95% credible interval.

Fig. S2. Variation in the posterior parameter distribution quantiles (median and bounds of the 95% Bayesian credible interval) as a function of the number of simulations ($N_{sim}$), for (a) Model 1 (random return), (b) Model 2 (nearest return) and (c) Model 3 (distance-based return probability). The error bars show the 95% central range for each estimate and were obtained from 100 bootstrap replicates at each value of $N_{sim}$.

**Figure S1(a)**

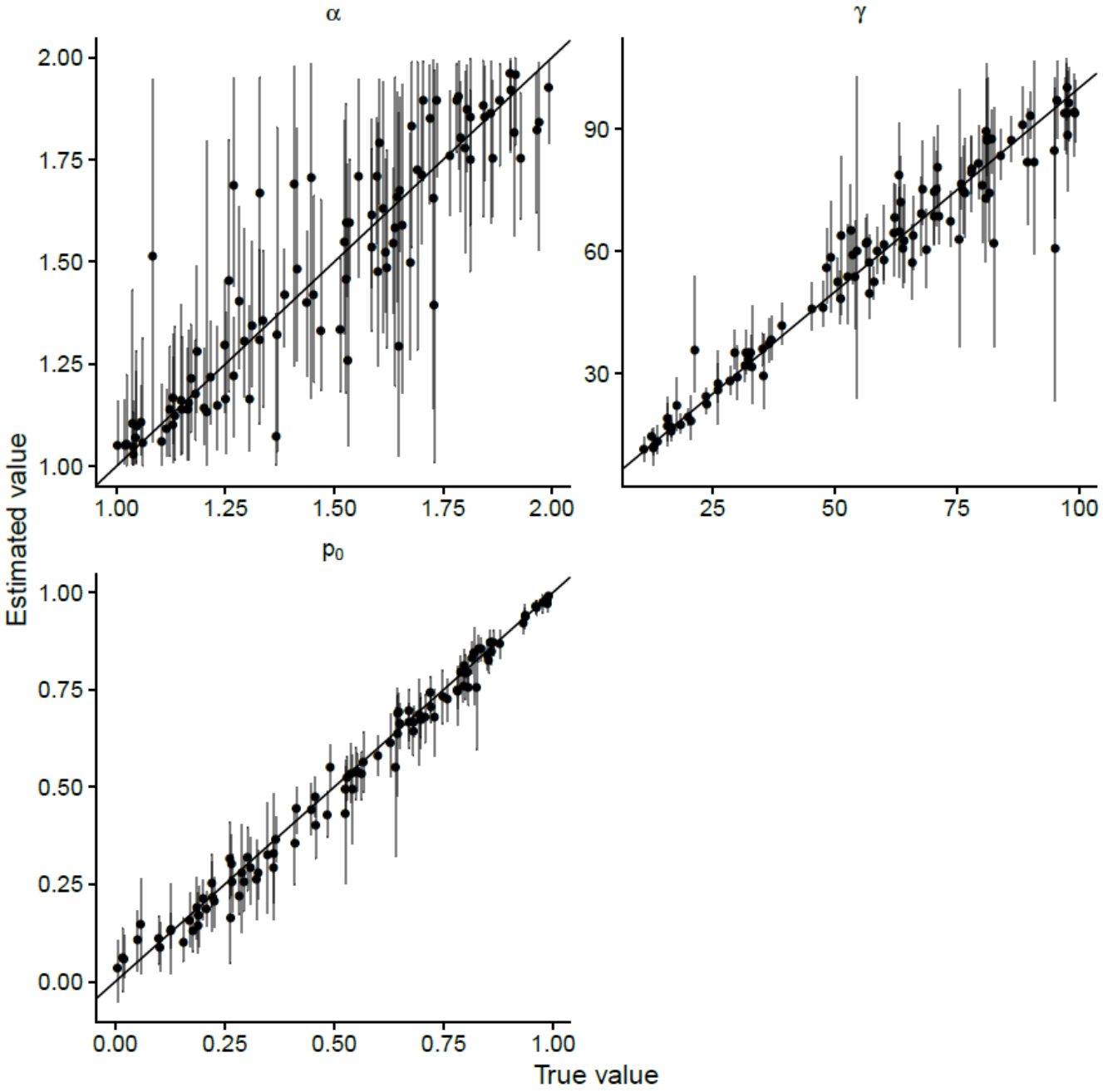
α
γ
p0
Estimated value
True value
2.00
1.75
1.50
1.25
1.00
90
60
30
25
50
75
100
0.75
0.50
0.25
0.00

**Figure S1(b)**

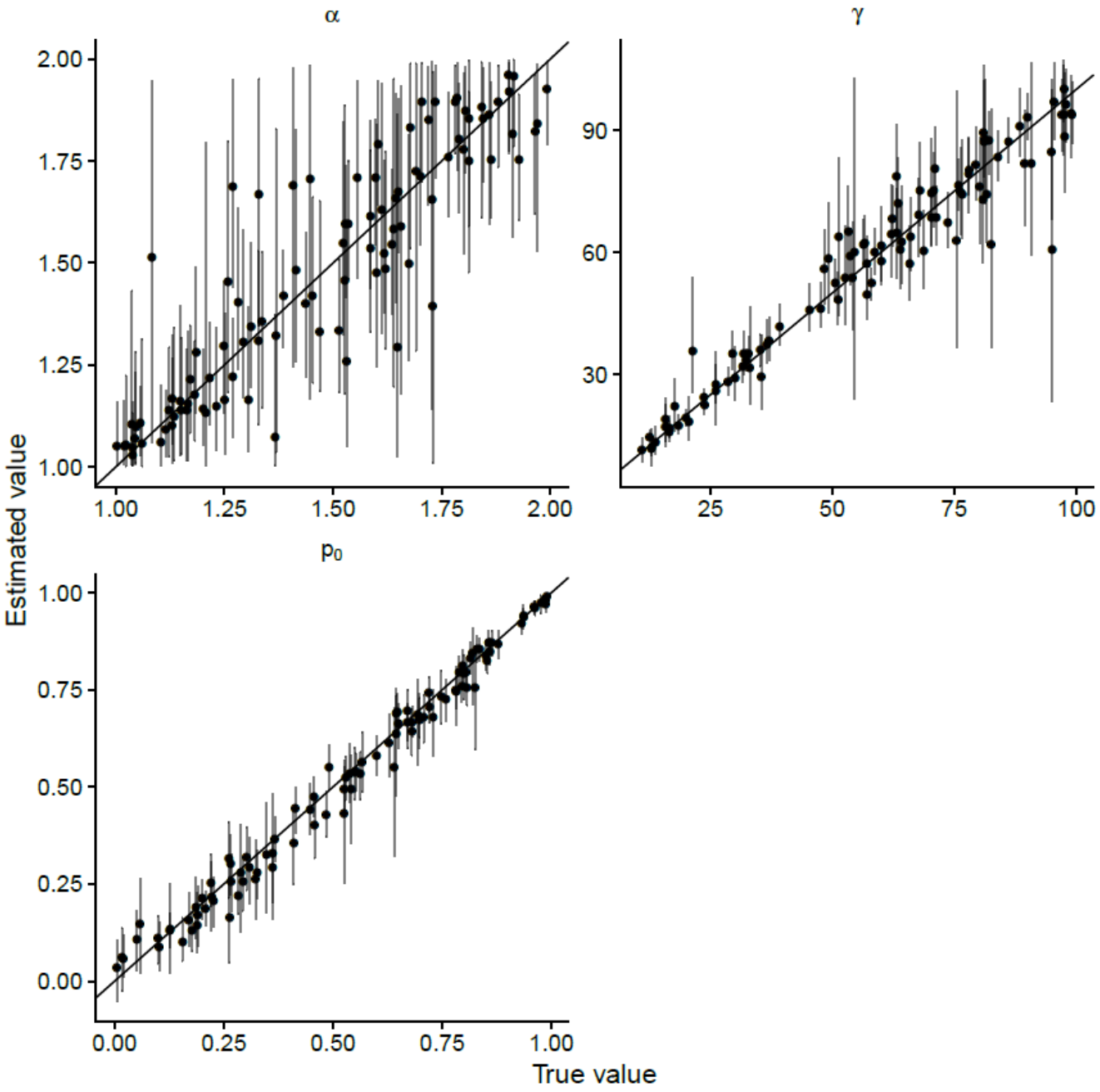
α
γ
p0
Estimated value
True value
2.00
1.75
1.50
1.25
1.00
90
60
30
25
50
75
100
0.75
0.50
0.25
0.00

**Figure S1(c)**

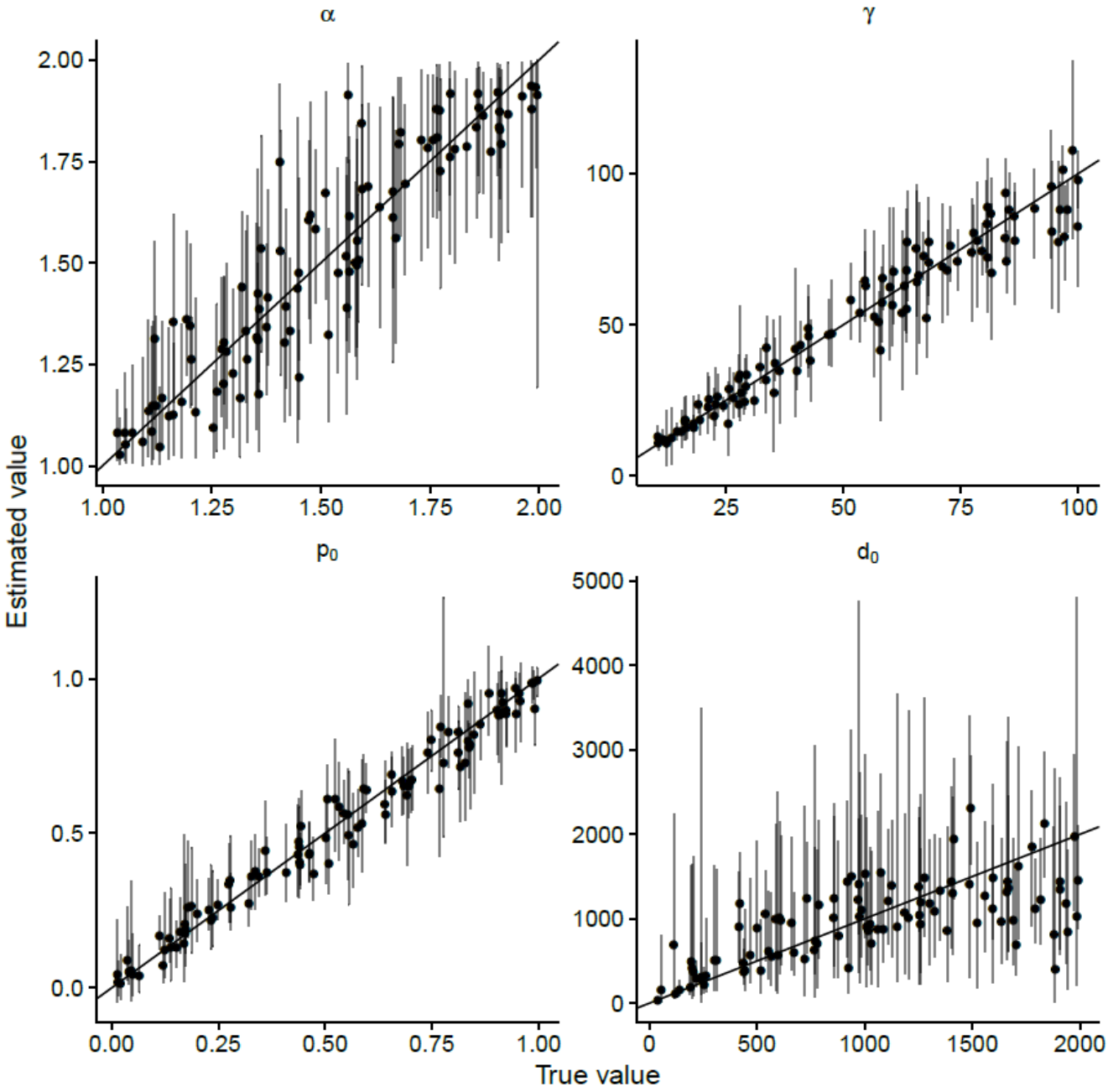
α
γ
p0
d0
Estimated value
True value
2.00
1.75
1.50
1.25
1.00
100
50
0
25
50
75
100
1.0
0.5
0.0
0.00
0.25
0.50
0.75
1.00
5000
4000
3000
2000
1000
0
500
1000
1500
2000

**Figure S2(a)**

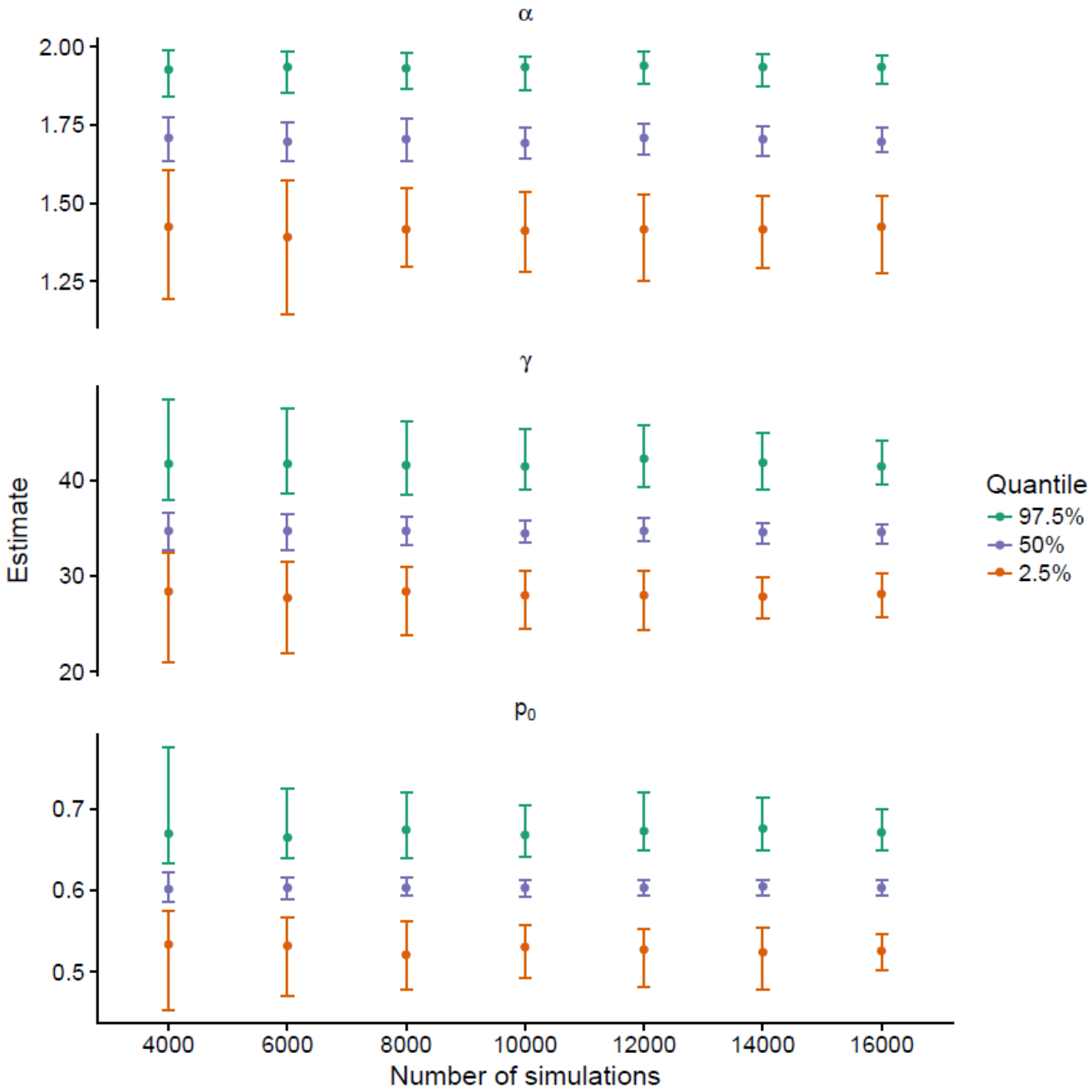
α
2.00
1.75
1.50
1.25
γ
40
30
20
Estimate
p0
0.7
0.6
0.5
4000
6000
8000
10000
12000
14000
16000
Number of simulations
Quantile
97.5%
50%
2.5%

**Figure S2(b)**

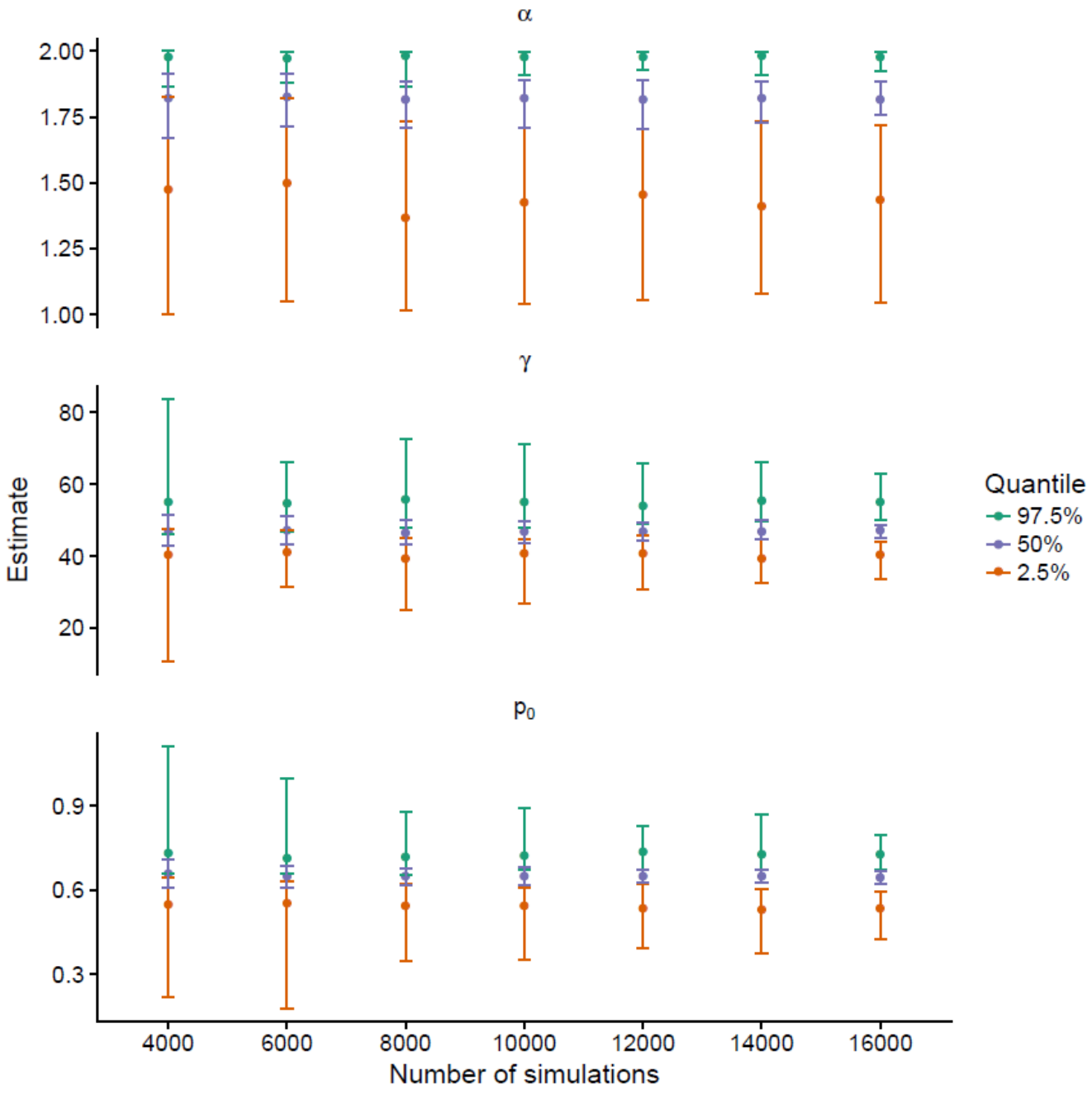
α
2.00
1.75
1.50
1.25
1.00
γ
80
60
40
20
Estimate
p0
0.9
0.6
0.3
4000
6000
8000
10000
12000
14000
16000
Number of simulations
Quantile
97.5%
50%
2.5%

**Figure S2(c)**

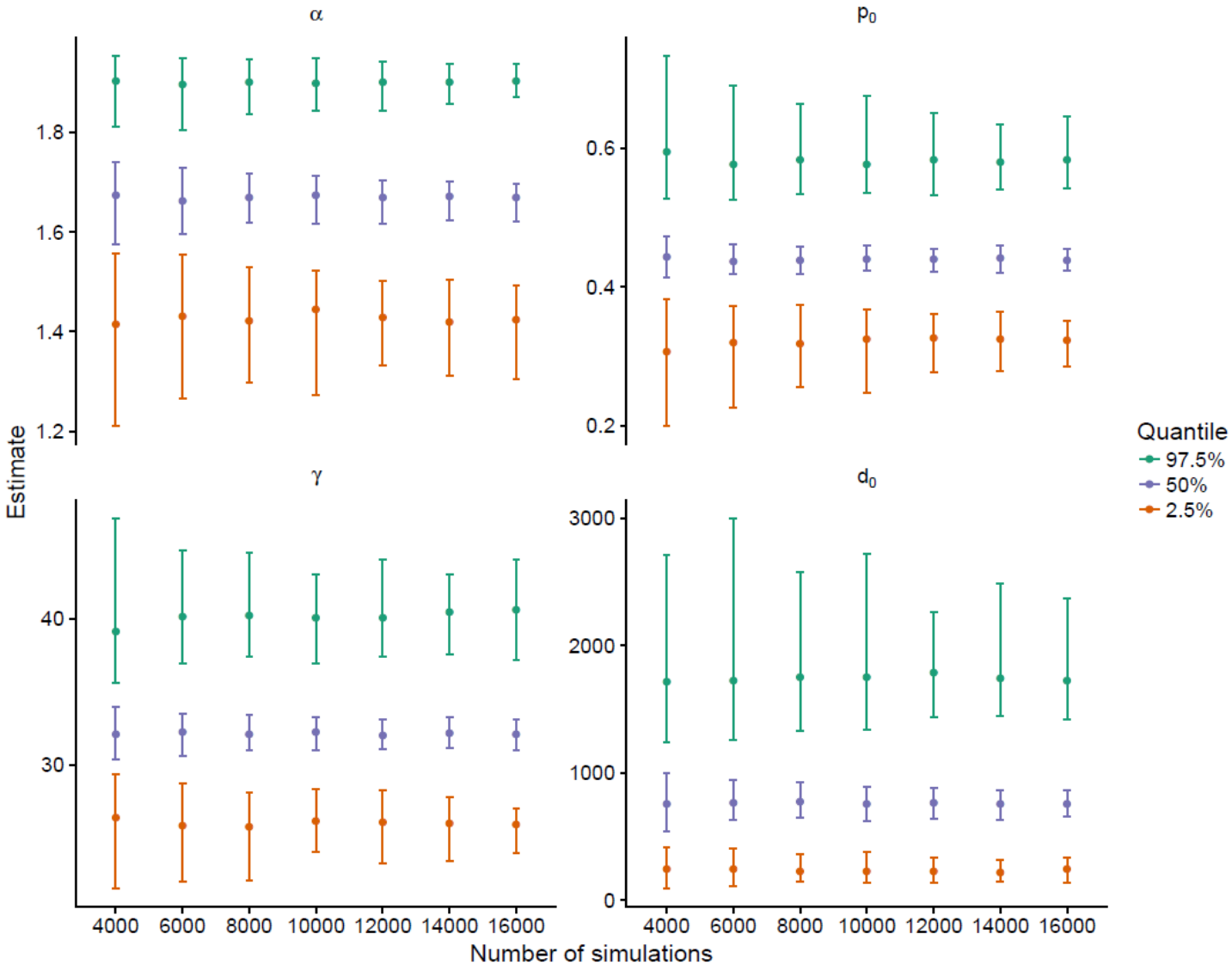
α
p0
γ
d0
Estimate
Number of simulations
Quantile
97.5%
50%
2.5%
1.2
1.4
1.6
1.8
0.2
0.4
0.6
30
40
0
1000
2000
3000
4000
6000
8000
10000
12000
14000
16000